Desalination 518 (2021) 115277

Contents lists available at ScienceDirect

Desalination

journal homepage: www.elsevier.com/locate/desal

Fouling fractionation in reverse electrodialysis with natural feed waters demonstrates dual media rapid filtration as an effective pre-treatment for fresh water

Bárbara Vital [a,b], Eduardo V. Torres [a], Tom Sleutels [a], M. Cristina Gagliano [a], Michel Saakes [a], Hubertus V.M. Hamelers [a,b,*]

[a] Wetsus, European Centre of Excellence for Sustainable Water Technology, Oostergoweg 9, MA 8911 Leeuwarden, the Netherlands
[b] Environmental Technology, Wageningen University and Research, Bornse Weilanden 118, 6708 PD Wageningen, the Netherlands

HIGHLIGHTS

- Dual media rapid filtration is a simple yet effective pre-treatment method for reverse electrodialysis applications
- Particles with average diameter of 10 μm in fresh water caused ~25% reduction in gross power density over 54 days operation
- Further pre-treatment with microfiltration allowed the development of a polysaccharidic lattice of EPS on membrane surface
- Biofouling lead to a reduction of only ~3% in gross power density over 54 days

ARTICLE INFO

Keywords:
Reverse electrodialysis
Natural water
Fouling
Renewable energy
Rapid filtration

ABSTRACT

Reverse electrodialysis (RED) is a process to harvest renewable energy from the salinity gradient obtained by the controlled mixing of river and seawater. When using natural waters, (bio)fouling is an inevitable process which has a negative impact on the obtained power density. Specific characteristics of RED do not allow the direct transfer of knowledge from previous fouling studies in other membranes process. More insight on how fouling is impacting RED is needed to design effective pre-treatment solutions. In this study, fresh water was fractionated based on particle size for 54 days, revealing the impact that specific foulants have on the RED process. A combination of turbidity and particle size measurements coupled with stack performance throughout the experiment showed that particles with an average diameter of 10 μm are responsible for a reduction in obtained stack power density of around 25%. Visualization of extracellular microbial polymers by confocal laser scanning microscopy confirmed that the role of biofouling only was of lesser concern compared to the impact of these suspended particles. According to these results, the removal of suspended particles >10 μm using a dual media filter has shown to be a simple and effective pre-treatment for fresh water in RED applications.

1. Introduction

In the last decades, Salinity Gradient Power (SGP) – also called Blue Energy – has been receiving substantial attention as an alternative renewable energy source. Reverse electrodialysis (RED) is a technology that can harvest the potential of SGP in river estuaries and turn it into electrical energy [1]. In RED a fresh and a saltwater stream are separated by ion-exchange membranes, and the concentration difference between the two water streams results in an electrochemical potential difference over the membranes [1–4]. This potential difference can be harvested when the ions selectively move through ion-exchange membranes, i.e. anions through anion exchange membrane (AEM) and cations through cation exchange membranes (CEM). The ionic current can be converted into an electrical current via redox reactions, and harvested if an external load is connected [1,5].

Since 1954, RED has been studied with model synthetic solutions with promising results [6,7]. However, there is a lack of studies focussing on fouling issues when using natural waters in RED systems [3,4]. Membrane fouling is a phenomenon resulting from the joint action of foulants depositing on the membrane surface [8,9], lowering the power

* Corresponding author at: Environmental Technology, Wageningen University and Research, Bornse Weilanden 118, 6708 PD Wageningen, the Netherlands.
E-mail address: bert.hamelers@wur.nl (H.V.M. Hamelers).

https://doi.org/10.1016/j.desal.2021.115277
Received 16 April 2021; Received in revised form 2 July 2021; Accepted 26 July 2021
Available online 10 August 2021

generation [4,5]. Natural waters contain a variety of compounds that can cause fouling, namely fine particles, colloids, microorganisms and (in)organic compounds [4,8]. One of the main effects of fouling is an increase of pressure drop over a stack's feed compartment, resulting in a higher energy consumption to pump the feed waters through the stacks. This increased energy consumption leads to a reduction of the overall net power density produced by the RED process [2,5,10,11]. Fouling can also include the clogging of the inlets' feed compartments, which affects flow distribution inside the stack and can reduce the obtained power density [10]. Finally, fouling of the ion-exchange membranes can hinder ion transport and thereby increases the internal resistance of the stack, reducing the power density that can be harvested [2].

Substantial knowledge about fouling is available for pressure driven membranes processes like e.g. ultrafiltration or reverse osmosis [12]. As RED is not a pressure driven process, the mass transport phenomena are different and different fouling processes and effects can be expected. Electrodialysis (ED) is a process that shares more similar characteristics with RED and its fouling has been studied in more detail; however there are still substantial differences in configuration between the two processes, such as larger intermembrane distance, opposite current direction and higher current densities for ED [13,14]. These differences do not allow for a direct transfer of fouling knowledge from ED to RED applications. Furthermore, in RED two types of ion exchange membranes are in contact with the two different water streams, resulting in four different combinations of natural water and ion exchange membranes and therefore four different types of fouling interactions need to be understood. Fig. 1 outlines the possible fouling interactions of membranes process including RED and highlights the complexity for describing and understanding the fouling in RED and the need to distinguish the different fouling interactions.

Overall RED performance is usually characterized using two types of measurements: pressure drop over inlet and outlet of each water compartment and electrochemical measurements derived from stack voltage and current. The first measurement gives an indication of fouling from each specific water stream, as it is measured for every compartment separately. The second measurement only gives an overall indication of the electrical performance as it can only be measured for the full stack and therefore does not allow separating the source of the fouling. For a full evaluation of the four possible interactions of fouling, a membrane autopsy is needed.

Fouling in RED applications using natural waters depends on intricate physical and chemical interactions between diverse compounds in the waters and the chemical groups on membrane and spacer surfaces [8,9]. Previous studies have shown that the possible four interactions can result in distinctive types of fouling. For example, the combination of seawater and CEM can possibly lead to scaling, due to higher concentration of multivalent ions in the seawater compartments that can precipitate on the membrane surface [2]. The combination of fresh water and AEM is known for the incidence of organic and colloidal fouling, since these compounds are present in relevant concentrations in fresh water and are mostly negatively charged [2,9,15]. Clay particles are also negatively charged and thus more prone to cause fouling in AEMs than in CEMs [2,3]. The four possible interactions in RED should be studied separately in order to propose adequate measures for fouling control.

Feed water composition is a key factor determining fouling and therefore impacting the power output of the RED process [16]. Previous studies on water composition and fouling with synthetic solutions showed to which extend certain foulants would impact RED performance, mostly investigating the effect of multivalent ions and model organic compounds, such as humic acids (HA) and sodium dodecyl benzene sulfonate (SDBS) [17,18]. These compounds caused fouling and uphill transport of ions, increasing membrane resistance and significantly impacting the obtained power density [4,17,18]. In the work of Post et al. [19], the effect of biofouling and mitigation measures to prevent biofouling were studied. They used sodium chloride and nutrient rich solutions inoculated with natural waters as feed and results showed a steep increase of pressure drop, resulting in a loss of performance, even after applying measures to mitigate biofouling. Unfortunately, these findings can hardly be translated into the real world, as natural waters entering the RED stacks are a mixture of potential foulants (ranging from soluble compounds to particulate matter) that can interact in unpredictable ways. The main foulants usually found in surface waters (both fresh and salt) are the following [8]:

- Particulate matter: inorganic or organic suspended particles and aggregates usually in the size range of micrometres that can block membrane surface. The most common found in surface water are silt, clay, precipitated iron and aluminium oxides and silicates, organics aggregates and cellular debris. Suspended particulate matter size in fresh water bodies usually varies between 1 and 100 μm, with peak concentrations around 30 μm [20,21].
- Organic: dissolved components and colloids, such as humic and fulvic acids, or extracellular polymers produced by algae or microorganisms, that can attach to the membrane surface by sorption interactions. Colloids are usually classified in the size range below 1 μm until 0.001 μm, and dissolved organic matter with molecular weight (MW) of 300-100,000 Da. These compounds originate of residues from decomposition of animal and plants and form a complex heterogeneous mixture. Humic substances usually account for more than 50% of this fraction in surface water, while proteins, amino acids and carbohydrates vary from 20 to 40%.
- Inorganic: mostly insoluble compounds, such as calcium carbonate ($CaCO_3$), calcium phosphate ($Ca_3(PO)_4$) and silica (SiO_2) or as well cations Mg^{2+}, Ca^{2+} that can precipitate on the membrane surface,

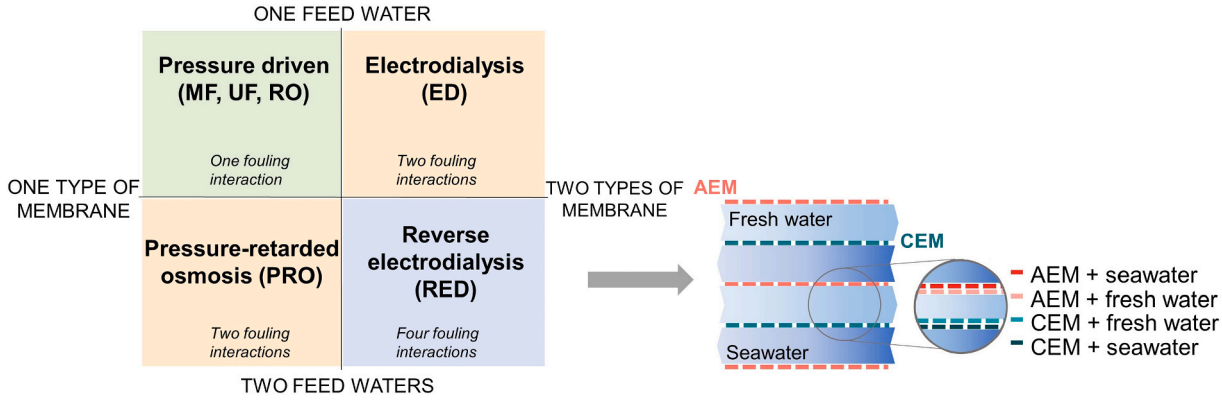

Fig. 1. Possible fouling interactions on various membranes process based on the different types of membranes and feed waters, and specification of possible fouling interactions on RED.

usually due to pH change or by concentrations exceeding their solubility.

- Micro-organisms and EPS (extracellular polymeric substances): mainly algae and microorganisms that can adhere to membranes and grow on top of these in the form of a biofilm. Biofilm is an aggregate of living and dead cells, embedded in EPS, which are polymeric substances excreted by active microorganism or present in aquatic systems in the form of mucus, slimes and lysis products [22]. EPS is rich in polysaccharides and proteins, forming the larger fraction of biofilms (50-80% of organic matter). In membrane processes, EPS from water can accumulate causing fouling phenomena, because of their ability to bind water, molecules and ions and thus alter the membrane functions.

On the basis of the above-mentioned classes of foulants found in natural waters, the goal of this work was to fractionate these and associate each fraction with variations in the performance of the RED process. For this purpose, a pilot-scale dual media rapid filter was used as pre-treatment for the influent natural water and then further fractionated with a micro cartridge filter. A dual media filter is considered environmental friendly and low energy-intensive, which are key characteristics for a pre-treatment on a RED system [23,24]. Analytical techniques were used to determine feed water quality and study the fractionated foulants. Foulants on the membrane surface were studied using microscopic techniques in membrane autopsies after the experiment was finished. The impact of the specific foulants was linked to the RED stack performance. This combination of performance measurements and water and membrane analysis aims to detect and understand and to possibly predict fouling in its distinctive and interrelated dimensions.

To the best of our knowledge, this is the first study addressing foulants phenomena in a RED process via natural foulants fractionation while a pilot scale dual media rapid filter is used as pre-treatment for RED. This approach gives insights in which components, among the whole spectrum found in feed waters, are the ones that affect the performance the most and in which way. This study is a fundamental approach and provides a knowledge base for designing future effective pre-treatments methods for RED processes.

2. Materials and methods

The experiment was performed in the Afsluitdijk Pilot Plant of REDstack BV (The Netherlands). Seawater (SW) was supplied from the Wadden Sea (Breezanddijk, The Netherlands) and fresh water (FW) from the IJsselmeer (The Netherlands) and the intake points are shown in Fig. S1.1.

2.1. Foulant fractionation setup

2.1.1. Feed waters pre-treatment

Fig. 2 displays a schematic representation of the set-up used in this study. Both fresh and seawater first went through a drum filter with a 20 μm pore size mesh, and then to a 30m^3 storage tank that was refilled continuously. After, the feed water passes through a dual media rapid filter pre-treatment, ending in the setup buffer tanks. Dual media rapid filters were composed of a 50 cm layer of anthracite (1.2–2.0 mm Ø) on top of a 50 cm layer of sand (0.5–1.0 mm Ø), placed into 11 cm Ø PVC pipe. Sand and anthracite were supplied by Filcom (SCR-Sibelco N.V., Belgium). The filters were individually backwashed twice a week by flushing with compressed air and processed water, for a minimum of 10 min or until no colour was seen in the effluent.

After the dual media filters, the two feed waters were further treated differently. The treatment of seawater aimed to remove as many foulants as possible, so the fouling incidences on the RED stack performances can only be associated to foulants coming from fresh water.

The river water pre-treatments aim to remove certain types of foulants in each fractionation step, so the performance of each stack can be attributed to the remaining foulants in their feed water. For this reason, stacks DM I and II (after dual media filtration - Fig. 2) received fresh water directly after the dual media rapid filter pre-treatment, while Stacks Micro I and II received fresh water after a step of micro-filtration with cut-off pore size of 1 μm (gradient cartridge filter DGD.2501.20, Pentair, The Netherlands). For seawater, the stream feeding all the stacks was pre-treated with the same micro-filtration cartridge, a granular activated carbon filter (GAC-10″, Pentair, The Netherlands) and finally an ultra-filtration module of 0.02 μm pore size (R-21 module, Pentair, The Netherlands). All stacks received their feed waters after their pre-treatment by using adjustable peristaltic pumps (Cole-Parmer,

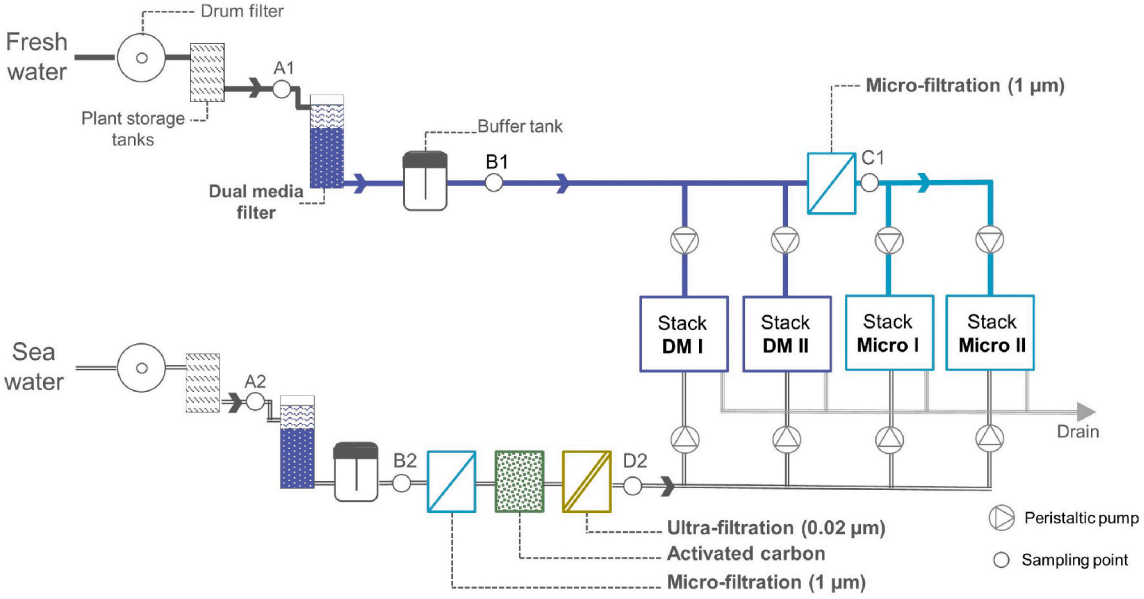

Fig. 2. Schematic representation of the experimental set-up in the Afsluitdijk pilot REDStack facility at Breezanddijk in the Netherlands. Fresh water passes a dual media rapid filter (stacks DM I and II) and a micro-filtration unit (1 *μm*) (stack Micro I and II). Sampling points A represent the effluent of the drum filters of the pilot plant, sampling points B the effluent of the dual media filtration, point C the effluent of microfiltration and point D the effluent of ultrafiltration.

Masterflex L/S Digital drive, USA).

Feed waters were characterized at six different sampling points every 3 days (detailed in Section 2.2). Three sampling points were established for each water stream (Fig. 2), where points A represent the feed waters in the beginning of the process, points B represent the waters treated after the dual media filter, point C represents the fresh water after microfiltration, and point D2 represents seawater after full treatment (last treatment is ultrafiltration). Point D2 was used as control for seawater that actually fed the stacks, but due to its extensive treatment, the detection limit of equipment and methods used to detect physicochemical characteristics was not reached, thus results are not shown. The experiment lasted for 54 days and membrane autopsy was performed afterwards (detailed in Section 2.3).

2.1.2. Stack configuration

Four 10 cm × 10 cm REDstack X-flow stacks were built in the lab with housing supplied by REDstack BV (Sneek, Netherlands). Stacks contained 10 cell pairs of flat CEM and AEM of the Fuji BE series (non-commercial membranes, Fujifilm Manufacturing Europe B.V., Netherlands), which membrane specifications are listed in Table 1.

Within each stack, membranes were separated by 480 μm woven netting spacers (PES 740/53, Saati S.p.A. Italy) and integrated silicon rubber (Deukum GmbH, Germany) acting as a sealer. Stacks were operated at 0.5 cm/s flow velocity and pressure drop over the outlet and inlet of the stacks was continuously measured by a pressure difference transmitter (EJA110E, Yokogawa, Japan). The electrolyte solution was composed of 0.05 M $K_3Fe(CN)_6$, 0.05 M $K_4Fe(CN)_6$ and 0.25 NaCl (VWR, USA) dissolved in Milli-Q water. The electrolyte compartments were shielded with an additional CEM and kept at an over pressure of 0.3 bar. At both sides of this membrane pile, titanium electrodes (mesh 1.7 m^2/m^2) with a galvanic platinum coating of 2.5 μm and with an active area of 10 cm × 10 cm were used as the anode and cathode (Magneto Special Anodes B.V., Netherlands). Temperature and conductivity of the feed waters after the buffer tank were measured using a sensor and recorded every 60 s using a data logger (GX10, Yokogawa, Japan).

2.1.3. Electrochemical measurements

Chronopotentiometric series were applied using a potentiostat (Iviumstat, Ivium Technologies, Netherlands) connected to a peripheral differential amplifier to measure voltage and calculate the open circuit voltage, stack resistance and gross power density, using the same well established method as described in [2,9]. The chronopotentiometry series consisted of constant current density steps of 4 A/m^2, 5 A/m^2, 6 A/m^2 and 7 A/m^2 applied for 60 s each – to reach a constant voltage value – which were separated by steps of 20 s with no current when the OCV was measured.

The rest of the time, the stacks were operated at constant current density of 5 A/m^2 to simulate a RED process.

2.2. Feed waters characterization

Feed waters were sampled at the sampling points (Fig. 2) and were subjected to diverse physicochemical analysis:

Ion concentration: relevant anion (Cl^-, Br^-, SO_4^{2-} and NO_3^-) and cation (Na^+, Ca^{2+}, K^+ and Mg^{2+}) concentrations were measured by ion chromatography (Metrohm Compact IC Flex 930, Schiedam, Netherlands).

Table 1
Membrane properties of cation and anion exchange membranes of Fujifilm BE series.

Membrane	Dry thickness [μm]	Permselectivity (0.05–0.5 M NaCl)	Electrical resistance (0.5 M NaCl) [Ω.cm2]
CEM BE	45	96%	1.42
AEM BE	53	94%	0.70

Organic carbon concentration was calculated by measuring total carbon (TC) and its fractions of total organic carbon (TOC) and inorganic carbon (IC) via a total organic carbon analyser (TOC-L, Shimadzu, Japan).

Concentration of particulate matter: total suspended solids (TSS) and volatile suspended solids (VSS) were determined using a standard protocol [25].

Particle size distribution: analysis performed using a particle size analyser DIPA-2000 (Donner Technologies, Netherlands).

Turbidity: analysis performed using the turbidimeter 2100 N IS (Hach, USA).

pH and conductivity: These parameters where monitored by using a calibrated bench top multi-parameter quantifier (Mettler Toledo, USA).

2.3. Membrane autopsy

Autopsy of the membranes was performed at the end of the experiment by opening the stacks and observation of samples was made using different microscopic approaches to visualize existing fouling. The cell pairs located in the centre of the membrane pile were sectioned in its central area for microscopic analyses (Fig. S3.1), described next.

2.3.1. Optical microscopy and EPS staining

To visualize if extracellular polymeric substances (EPS) were causing biofouling, the cut sections of each membrane were placed on a clean microscopy glass slide and stained with crystal violet 0.1% solution (Crystal Violet/ammonium oxalate solution, Boom B.V., Netherlands). Crystal violet was applied to visualize the organics (protein and carbohydrates) of EPS [26]. After 30 min of staining, samples were washed with Milli-Q and then observed with phase contrast microscopy (Leica DM750, Leica, Switzerland) at 10, 20 and 40× magnification. Images were taken using the software LAS 4.12 (Leica, Switzerland).

2.3.2. Fluorescent staining and Confocal scanning laser microscopy (CSLM)

A further characterization of the EPS fraction of fouling layers was carried out by applying fluorescent staining of proteins and carbohydrates. Sections of the membranes were placed on a 6-well plate and first treated with calcofluor white (CW) (Sigma-Aldrich Chemie B.V., Netherlands) for visualization of β-polysaccharides, and subsequently with Sypro™ Red (Molecular Probes, Thermo Fisher Scientific, USA) for visualization of proteins. Both stainings were carried out for 60 min in the dark and after membrane sections were washed with PBS to remove excess dye. Finally, the membrane samples were observed with Confocal Laser Scanning microscopy (CSLM) via a Zeiss LSM 880 (Zeiss, Germany). Images were acquired through the software ZEN black (ZEISS, Germany).

Before the CLSM analysis, clean membrane supports were tested for fluorescence emission with the staining. Due to the slight negative charge of the dyes used in this study, they were interacting with the clean AEM membranes (Fig. S3.2), making impossible to apply this analysis on them.

2.3.3. Scanning electron microscopy (SEM) and energy-dispersive X-ray spectroscopy (EDX)

Sections of the membranes were placed on a 6-well plate and fixed in 2.5% glutaraldehyde overnight at 4 °C. After, they were rinsed twice with Milli-Q and dehydrated in graded ethanol solutions (30, 50, 70 and 90%) for 20 min each, and finally 99.6% ethanol was applied twice for 30 min. The samples were dried for 30 min at 55 °C before SEM analysis with a JEOL JSM-6480LV (JEOL, Japan) at an acceleration voltage of 6 kV and magnifications up to 30,000×. Identification and quantification of relevant chemical elements was carried out with energy dispersive X-ray detector (x-act SSD-EDX, Oxford Instruments, UK) coupled with the SEM imaging. The images were processed using JEOL SEM Control User Interface software (version 7.07).

3. Results and discussion

Fouling in the RED process using natural feed waters was studied by analysing the fractionated feed waters, looking at stack performance and membrane autopsy after the 54-day experiment.

3.1. Fractionation of feed water and their characteristics

The fractionation of fresh feed water and the sampling points are shown in Fig. 2. Each sample was characterized by its turbidity, Total Suspended Solids (TSS), average particles size, ion composition, and total carbon, inorganic carbon and total organic carbon (TOC) and the results are presented in Tables 2 and 3.

Turbidity, TSS and particle size, (Table 2) all show a reduction of suspended solids after each fractionation step for both fresh and seawater. From the turbidity values and average particle size, it is clear that dual media rapid filtration removes bigger particles (up to approximately 10 μm in fresh water and up to 6 μm in seawater) and microfiltration removes smaller suspended particles between 10 μm and 1 μm in diameter, as expected and based on the potential of removal of the selected filters. The dual media filter allows for a more constant number of suspended particles in the effluent when compared to the drum filter, as seen in lower standard deviation in the measurement related to the dual media filter (Table 2).

Over the 54 days of experiment, among the 15 samples of fresh water taken after the dual media filter, just two of them had a turbidity exceeding 10 NTU. This shows that dual media rapid filter treatment is a reliable method even considering natural variations in water turbidity. For comparison, a pressurized full-scale sand/dual media rapid filter with coagulation pre-treatment can deliver an effluent with turbidity lower than 1 NTU [23]. This shows that it is possible to achieve even better results with an automated full-scale filter in the future. Reduction in turbidity after microfiltration is also relevant, as most values are below 3 NTU, with only two samples being around 5 NTU. These turbidity values support that the suspended particles are removed in the fractionation steps.

Also, for seawater, dual media filtration shows promising results as pre-treatment, reaching an average effluent quality of 5 NTU with turbidity removal of 71%.

The two consecutive fractionation steps applied on the freshwater stream did not remove ions and organic/inorganic carbon, as shown by similar values for ions (sodium, calcium, magnesium, potassium, chloride, and sulphate) and TC, IC and TOC (Table 3). Notably, both dual media and microfiltration were not able to remove the organic carbon from the influent water, which can be related to the subsequent bio- and organic fouling of the membranes.

Table 2
Physicochemical characteristics of fresh (1) and sea (2) feed water samples from the Afsluitdijk Pilot Plant. Sampling point A is the effluent of the drum filter and influent of the dual media filter, sampling point B is the effluent of the dual media filter and influent of microfiltration, and sampling point C is the effluent of microfiltration.

	Fresh water			Seawater	
Parameter	Influent dual media A1	Effluent dual media B1	Effluent Micro filter C1	Influent dual media A2	Effluent dual media B2
Turbidity (NTU)	12.2 ± 5.5	6.8 ± 3.6	2.5 ± 0.6	22.1 ± 13.2	5.0 ± 3.1
TSS (mg/L)	34.9 ± 21.3	14.6 ± 4.4	*	78.4 ± 19.3	31.3 ± 8.6
Average particle size (μm)	18.2 ± 4.5	10.4 ± 2.4	*	21.9 ± 5.0	6.4 ± 2.5

* Values below detection range.

Table 3
Chemical characteristics of fractionation of fresh (1) and sea (2) water from the Afsluitdijk Pilot Plant. Sampling point A is the effluent of the drum filter and influent of the dual media filter, sampling point B is the effluent of the dual media filters and influent of microfiltration, and sampling point C is the effluent of microfiltration.

	Fresh water			Seawater	
Parameter (in mg/L)	Influent dual media A1	Effluent dual media B1	Effluent Micro filter C1	Influent dual media A2	Effluent dual media B2
Sodium	86.0 ± 8.1	100.8 ± 9.3	119.3 ± 18.9	6534 ± 332	6485 ± 352
Calcium	44.8 ± 3.4	46.3 ± 3.0	43.4 ± 4.9	271.7 ± 11.1	273.6 ± 14.1
Magnesium	14.2 ± 0.7	16.0 ± 1.1	22.1 ± 13.3	779.3 ± 38.8	777.3 ± 42.4
Potassium	6.4 ± 0.4	7.0 ± 0.4	14.1 ± 10.8	241.2 ± 32.3	234.5 ± 28.0
Chloride	146.5 ± 13.7	172.8 ± 16.5	187.5 ± 40.0	11,826 ± 604	11,768 ± 622
Sulphate	63.2 ± 3.4	67.9 ± 3.6	57.8 ± 8.9	1695 ± 78	1685 ± 85
Total carbon (TC)	31.1 ± 0.9	32.1 ± 0.9	30.2 ± 0.8	38.6 ± 4.0	39.2 ± 6.4
Inorganic carbon (IC)	21.5 ± 3.0	23.5 ± 1.0	22.5 ± 1.0	27.5 ± 4.2	27.1 ± 4.0
Total organic carbon (TOC)	7.7 ± 0.6	7.9 ± 0.7	7.7 ± 0.5	8.4 ± 3.2	7.8 ± 3.7

3.2. Stack performance is mostly impacted by suspended particles

Stack performance is evaluated by pressure drop over the inlet and outlet of feed waters in the stack, internal stack resistance and gross power density obtained from the process. These measurements allow the assessment of eventual fouling and enable comparison with previous studies.

3.2.1. Pressure drop

The pressure drop between inlet and outlet of fresh water during the 54 days of experiment is presented in Fig. 3. An increase in pressure drop was observed approximately one month after the start of the experiment. By the end of the experiment (day 54), a clear difference in pressure drop can be seen for the stacks after the dual media filter (80 mbar) when compared to the stacks after microfiltration (20 mbar) (Fig. 3). This shows that the microfiltration pre-treatment can lead to a lower build-up of fouling in long term operation. This comes with the expense of additional treatment procedure.

As all chemical parameters do not significantly change in the fractionation steps (Table 3), the differences in stack performance can relate to the fouling due to particles with average diameter of 10 μm or lower, which are passing through the dual media rapid filter. Therefore, the highest impact on performance is caused by suspended particles. This is also the case for other parameters that determine the stack performance (internal resistance and gross power density) presented in the next section. Even though the rapid filter reduces fouling significantly when compared to the 20 μm mesh drum filters, the dual media filter effluent still contains a relevant amount of foulants, which still impacts the performance in the long term.

The values of pressure drop in stacks DM I and II, without applying any cleaning strategy, are very low when compared to other pre-treatment methods used before. For example, Vermaas et al. 2013 reached around 1.5 bar with fresh water after 25 days of operation when using only a drum filter of 20 μm mesh as pre-treatment and stacks with intermembrane distance of 240 μm. Moreno et al. (2017), using the same pre-treatment, reported a total pressure drop increase, accounting for both fresh and sea water, of around 900 mbar and the stack had to be stopped after 45 days of operations, due to this high pressure drop. In the

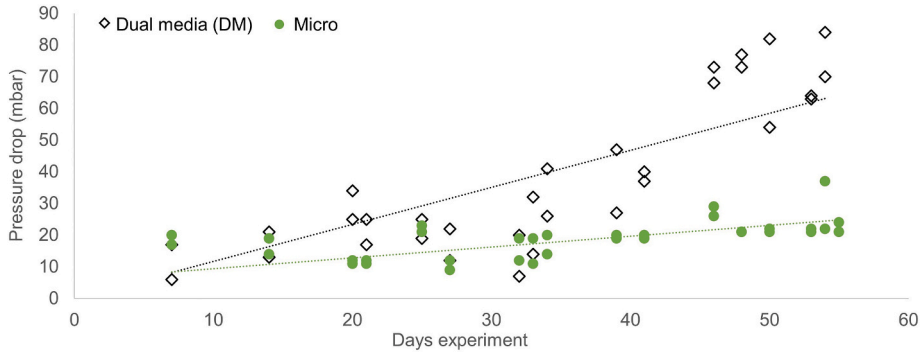

Fig. 3. Pressure drop measurements for fresh water flow through stacks after dual media filtration (in black) and microfiltration (in green). Duplicate measurements are shown as markers and the linear regression of the average of the two measurements are represented as lines ($R^2 = 0.719$ for DM stacks and $R^2 = 0.624$ for Micro stacks).

present study the contribution of seawater to the pressure drop is low (<10 mbar), since this stream is fully treated, resulting in a total pressure drop of 90 mbar (considering fresh and seawater streams).

3.2.2. *Internal stack resistance and gross power density*

The initial and final internal stack resistance and gross power density for the two fractionation steps of fresh water are presented in Fig. 4 and the extended data over time is presented in Fig. S2.1. This stack resistance was corrected for the resistance associated with the conductivities of waters and therefore only represents the resistance of the membranes and associated fouling in the stack.

The internal resistance of all stacks in the beginning of the experiment was comparable, around 8 Ω (Fig. 4). By the end of the experiment, the stacks after the dual media filtration step reached an average of 10.8 Ω, an increase of about one third of the initial value. For the stacks after the microfiltration step, the average resistance was 9.3 Ω, representing an increase of around 15% of the initial value. This increase in resistance can be attributed to fouling of the spacers and membranes, as other conditions were unchanged. The increase in resistance of the stack after the microfiltration is around half of the increase of stacks receiving fresh water pre-treated with dual media filtration, and according to water samples and membrane autopsy the fouling in those stacks is mostly from organic soluble colloids and EPS. Thus, these compounds influence the performance of the stacks to a lower extent than particulate matter.

The gross power density and the internal resistance are inversely related, thus an increase of internal resistance corresponds to a decrease in gross power density, [5]. In the initial stage of the experiment, the power density of the stacks fed with dual media filtered and micro filtered freshwater was comparable (0.20–0.21 W/m^2). The exception was one of the stacks after dual media filter fractionation (stack DM II), which after the first day of the experiment had a lower OCV (resulting in 0.16 W/m^2 after applying a load), probably due to an internal leakage. During the experiment, performance stabilized with a slightly lower value of OCV and gross power density than the other stacks (DM I, Micro I and II).

As observed in the previous sections, stacks DM I and II suffered a higher impact in performance due to fouling compared to the ones after microfiltration. This translated in a reduction of 25% of gross power density in these stacks, while only a small reduction of 3% was registered after the microfiltration step. Of course, this comes with the investment of an additional treatment.

Still, the performance of the stacks receiving the water treated with dual media filtration is promising. The increase in resistance (~35%) is lower compared to previous studies. For example, Vermaas et al. 2013 reported an increase in resistance of 70% in 25 days when using a drum filter as pre-treatment and stacks with spacers (240 μm), while stacks with profiled membranes showed an increase of 40% in 25 days. The power density in the same study varied between 0.05 and 0.14 W/m^2, with the best results for stacks with profiled membranes. Moreno et al. (2017) compared cleaning strategies for fouling removal and performance recovery and the best results were achieved with flushing CO_2, which reached a power density of 0.17 W/m^2 after 55 days of operations.

When dual media filtration is applied as pre-treatment, a similar performance (power density of 0.16 W/m^2) could be achieved as with profiled membranes or cleaning with CO_2. This shows the robustness of this pre-treatment and the potential it has to put Blue Energy in a better competing position with other sustainable energy sources.

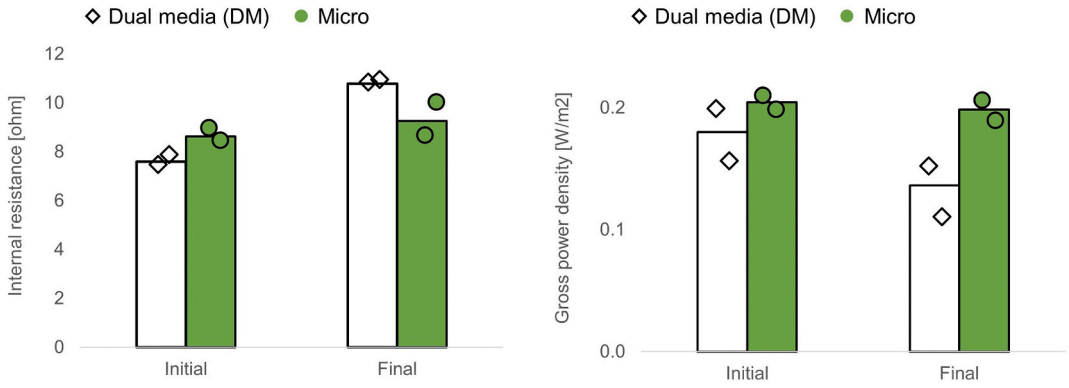

Fig. 4. Internal resistance of the stacks and gross power density at the initial and final stage of the experiment after dual media and micro fractionation step. Duplicate measurements are shown as dots and the average of the two measurements is represented as bars.

3.3. Membrane autopsy reveals particulate fouling after dual media filtration and biofouling after microfiltration

At the end of the experiment (day 54) membrane samples were taken from the stacks and were prepared for visual analyses, and representative pictures are shown in Fig. 5. AEMs were covered by a brown coloured layer (Fig. 5B and D), which was not observed for the CEMs (Fig. 5C and E) and can be attributed to the presence of humic acids. The negative charge of humic acids favours its attachment to AEMs which are positively charged, as reported before [2,3].

Particulate fouling was observed on both membrane types on stacks DM I and II (Fig. 5B and D) but not after the microfiltration step (Fig. 5C and E). The same can be seen for the spacers, where more particulate fouling accumulated after dual media filtration than after microfiltration (Fig. S3.3A and B).

To identify organic components in the fouling layers, first crystal violet was used as a fast method to stain the EPS present on the membrane (Fig. S4). Floccular EPS accumulated in some spots on the AEM and CEM of stacks DM I and II (Fig. S3.4A and B) and Micro I and II (Fig. S3.4C and D). This EPS could have originated either from accumulation from the feed waters, where it can be present as excretion or mucus or from microbial secretion, after cells attachment and growth on the membranes [22]. The amount and morphology of EPS fouling looked similar for both the membranes after the two different treatments (Fig. S3.4), as expected since organic polymers and cells were present in the feed water even after 1 μm filtration. EPS presence was further evaluated by the application of two fluorescent dyes targeting EPS main components, namely proteins (with SyproRed, in red) and polysaccharides (with CW, in blue). These dyes were applied on CEM membrane sections, and stained sections were analysed using confocal microscopy (Fig. 6).

CLSM images of CEM membranes showed the presence of EPS after both fractionation steps although with a different structural pattern (Fig. 6A to D). After the dual media filtration step, most of the EPS and cell structures detected were rich in proteins (red signal, Fig. 6A and B). The most common pattern detected were coccoid cells clustered to form aggregates near the membrane support fibres (Fig. 6A and B). Majority of the detected cells were positive to SyproRed, while polysaccharides were rarely detected, and always in combination with proteins (purple signal, Fig. 6B) mostly surrounding biological structures resembling nematodes and fungi (Figs. 6B and S3.5 A). On the other hand, EPS in stacks Micro I and II seems to be connected with the formation of a lattice rich in polysaccharides (Fig. 6C and D, purple signal) with a linear pattern, which was not observed on the membranes of stacks DM. The presence of a polysaccharides lattice, forming a network of linear junctions, could be related to the attachment and growth of different sort of cells [27] in comparison to the ones observed in stacks DM I and II (Fig. 6A and B). Since it was not possible to analyse AEM membranes via CLSM, these were analysed via SEM, and similarities could be observed with the respective CEM counterpart. Indeed, AEMs from DM stacks presented EPS/biofouling as little coccoid cells (Fig. 6E), and EPS aggregates (Fig. 6F). This EPS aggregates often contained diatomic reminiscent and other particles (Fig. S3.5B). Interestingly, a likely polysaccharides lattice pattern was visualized also in AEM after microfiltration (Fig. 6G) together with grouped cells (Fig. 6H). Combined CLSM and SEM results thus, unlike crystal violet staining (Fig. S3.4), highlighted a different shape of fouling after dual media and microfiltration treatments (Fig. 6). Different kind of cells were attaching and growing on top of CEM and AEM after the two pre-treatment steps, likely the result of a selection of certain types of microorganisms by the microfiltration step [28]. It is possible that the microorganisms that are able to pass the microfiltration step find less competition and more space to grow on the available membrane surface [29]. Another reason why we do not observe the same pattern observed in Micro stacks as in DM stacks could be related to the presence of particulate fouling (as clearly observed in Fig. 5) on the membrane surface. The adhesion of particles to the membrane surface form a sort of protective layer to bacterial adhesion, since it creates a less ideal surface for microbial growth [30]. Most probably the difference in EPS and biofouling is a combination of these two factors.

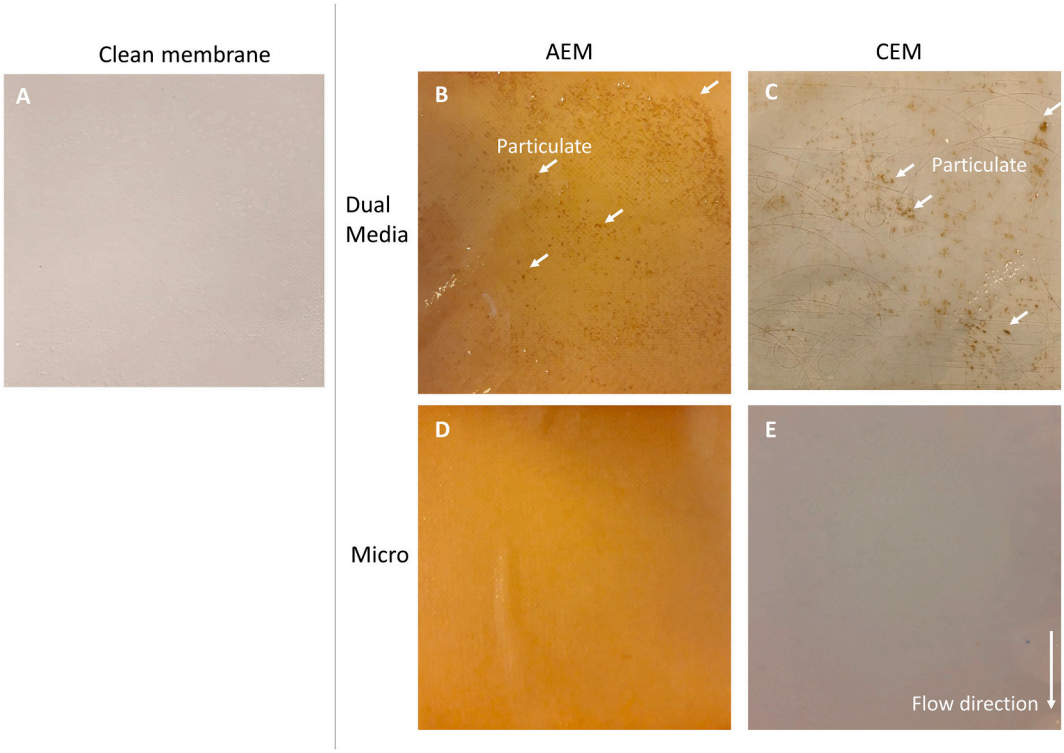

Fig. 5. Visual analysis of membranes (B to E) in contact with fresh water after 54 days experiment. For comparison, a clean membrane is shown (A), with no visual distinction between a clean AEM and CEM.

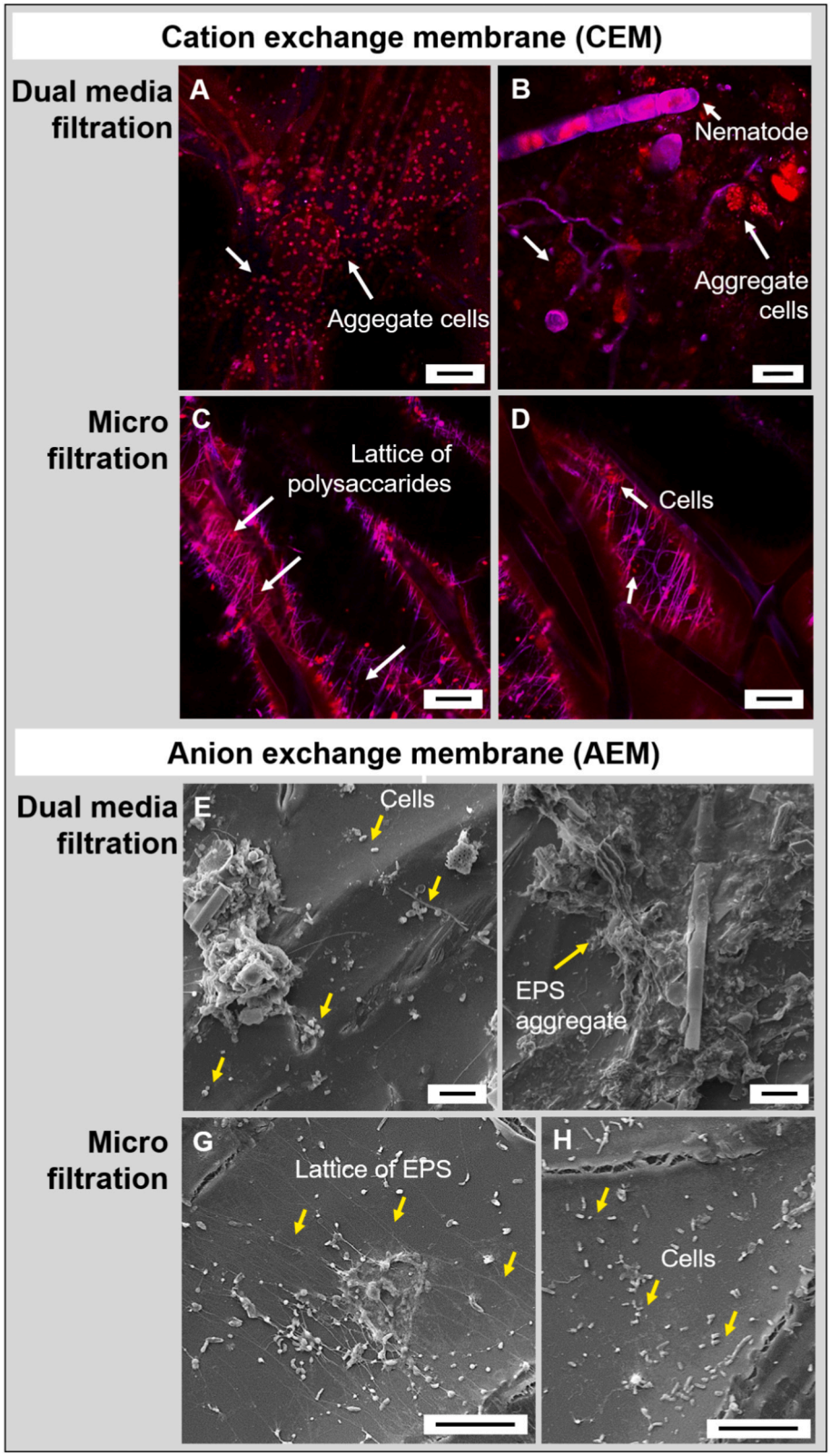

Fig. 6. Microscopic images of the biofouling developed on CEM and AEM analysed via CLSM and SEM, respectively. From A to D, CLSM dataset showing the combination of SyproRed (proteins, in red), and Calcofluor White (polysaccharides, blue). Purple indicates co-localization of the two staining signals, while white arrows indicate details. Stacks DM showed aggregate cells with a proteic outer layer adhering on the CEM membranes (A, B). In stacks Micro, biofouling was visualized as a lattice rich in polysaccharides, surrounding (C) and in within the membrane fibres, together with cells (D). From E to H, SEM images of AEM after fixation and dehydration. Yellow arrows indicate details. In stacks DM, cells (E) and EPS aggregates (F) were visualized. In stacks Micro, a lattice of EPS (G) and many cells (H) were present. Scale bar is 10 μm.

The water analysis presented in Section 3.2 showed that there were no consistent differences in TOC levels in the feed waters entering the stacks and after the different fractionation steps. However, the results from the membrane autopsy and microscopic analysis showed that there were substantial differences in the structure of biofouling due to the fractionation process and therefore fractionation can have an impact on fouling characteristics, in turn affecting stack performance.

Although there is this indication of a microbial/EPS fouling on the membrane surface after the microfiltration step, process performance in terms of pressure drop, internal resistance and gross power density, indicates that the impact in the RED process is small in comparison to particulate fouling. Future studies with an even longer duration to allow

more development of biofouling might unravel in detail the effective role of such foulants on RED performance.

4. Conclusions and implications

The fractionation of foulants from natural waters leads to a better understanding how each type of foulant can affect the RED process. Suspended particles with average diameter of 10 μm are responsible for a reduction in stack performance of around 25% in gross power density after operation of 54 days without cleaning measures.

Membrane autopsy of the stacks shows the presence of a polysaccharidic lattice of EPS formed after microfiltration treatment with potential development of more complex biofouling on the membrane surface. However, their impact in performance as a foulant is of lesser concern than the suspended particles found after the dual media rapid filtration step.

More studies are needed to investigate the effect of specific foulants on RED performance, such as studying a fractionation step for removal of organics and testing fractionation of seawater, in order to understand if the similar dynamics apply to this type of water.

It was shown that the use of a dual media filter is a simple yet effective pre-treatment method for RED applications, considering freshwater feed, when compared to the use of a 20 μm drum filter. The possibility of backwashing this type of filter with only air and water is an ecological acceptable cleaning tool for blue energy since no aggressive chemical cleaning agents are needed. Also, the media material (sand and anthracite) are durable materials that do not need to be replaced often.

CRediT authorship contribution statement

B. Vital: Conceptualization, Methodology, Investigation, Visualization, Writing - original draft.

E. Vías: Investigation, Writing – original draft.

T. Sleutels: Conceptualization, Methodology, Supervision, Writing - review & editing.

C. Gagliano: Conceptualization, Methodology, Supervision, Writing - review & editing.

M. Saakes: Conceptualization, Supervision, Writing - review & editing.

H. Hamelers: Conceptualization, Supervision, Writing - review & editing.

Declaration of competing interest

The authors declare that they have no known competing financial interests or personal relationships that could have appeared to influence the work reported in this paper.

Acknowledgments

This research was performed in the cooperation framework of Wetsus, European Centre of Excellence for Sustainable Water Technology (www.wetsus.nl). Wetsus is cofounded by the Dutch Ministry of Economic Affairs and Ministry of Infrastructure and Environment, the European Union Regional Development Fund, the Province of Fryslân and the Northern Netherlands Provinces. This work is part of a project that has received funding from the European Union's Horizon 2020 research and innovation programme under the Marie Skłodowska-Curie Grant Agreement 665874. The authors thank the participants of the research theme “Blue Energy” for fruitful discussions and financial support and specially REDStack for their input and use of the facility in the Afsluitdijk. The authors also thank Emanuel Dinis for the help with EPS staining and CLSM analysis, John Ferwerda and Jan Jurjen Salverda for building the setup used in this experiment.

Appendix A. Supplementary data

Supplementary data to this article can be found online at https://doi.org/10.1016/j.desal.2021.115277.

References

[1] J.W. Post, J. Veerman, H.V. Hamelers, G.J. Euverink, S.J. Metz, K. Nymeijer, C. J. Buisman, Salinity-gradient power: evaluation of pressure-retarded osmosis and reverse electrodialysis, J. Membr. Sci. 288 (2007) 218–230.
[2] D.A. Vermaas, D. Kunteng, M. Saakes, K. Nijmeijer, Fouling in reverse electrodialysis under natural conditions, Water Res. 47 (2013) 1289–1298.
[3] T. Rijnaarts, J. Moreno, M. Saakes, W.M. de Vos, K. Nijmeijer, Role of anion exchange membrane fouling in reverse electrodialysis using natural feed waters, Colloids Surf. A Physicochem. Eng. Asp. 560 (2019) 198–204.
[4] S. Pawlowski, R.M. Huertas, C.F. Galinha, J.G. Crespo, S. Velizarov, On operation of reverse electrodialysis (RED) and membrane capacitive deionisation (MCDI) with natural saline streams: a critical review, Desalination 476 (2020), 114183.
[5] J. Moreno, N. de Hart, M. Saakes, K. Nijmeijer, CO2 saturated water as two-phase flow for fouling control in reverse electrodialysis, Water Res. 125 (2017) 23–31.
[6] Signe Kjelstrup, Torleif Holt, Liv Fiksdal, Effect of biofilm formation on salinity power plant output on laboratory scale, in: Industrial Membrane Processes 82, 1986, pp. 39–44.
[7] R.E. Pattle, Production of electric power by mixing fresh and salt water in the hydroelectric pile, Nature 174 (1954) 660.
[8] W. Guo, H.-H. Ngo, J. Li, A mini-review on membrane fouling, Bioresour. Technol. 122 (2012) 27–34.
[9] S. Mikhaylin, L. Bazinet, Fouling on ion-exchange membranes: classification, characterization and strategies of prevention and control, Adv. Colloid Interf. Sci. 229 (2016) 34–56.
[10] D.A. Vermaas, M. Saakes, K. Nijmeijer, Power generation using profiled membranes in reverse electrodialysis, J. Membr. Sci. 385–386 (2011) 234–242.
[11] J. Di Luque Salvo, A. Cosenza, A. Tamburini, G. Micale, A. Cipollina, Long-run operation of a reverse electrodialysis system fed with wastewaters, J. Environ. Manag. 217 (2018) 871–887.
[12] M.B. Dixon, S. Lasslett, C. Pelekani, Destructive and non-destructive methods for biofouling analysis investigated at the Adelaide desalination pilot plant, Desalination 296 (2012) 61–68.
[13] D.A. Vermaas, M. Saakes, K. Nijmeijer, Enhanced mixing in the diffusive boundary layer for energy generation in reverse electrodialysis, J. Membr. Sci. 453 (2014) 312–319.
[14] M. Vaselbehagh, H. Karkhanechi, R. Takagi, H. Matsuyama, Biofouling phenomena on anion exchange membranes under the reverse electrodialysis process, J. Membr. Sci. 530 (2017) 232–239.
[15] R.S. Kingsbury, F. Liu, S. Zhu, C. Boggs, M.D. Armstrong, D.F. Call, O. Coronell, Impact of natural organic matter and inorganic solutes on energy recovery from five real salinity gradients using reverse electrodialysis, J. Membr. Sci. 541 (2017) 621–632.
[16] E.H. Hossen, Z.E. Gobetz, R.S. Kingsbury, F. Liu, H.C. Palko, L.L. Dubbs, O. Coronell, D.F. Call, Temporal variation of power production via reverse electrodialysis using coastal North Carolina waters and its correlation to temperature and conductivity, Desalination 491 (2020), 114562.
[17] E.J. Bodner, M. Saakes, T. Sleutels, C. Buisman, H. Hamelers, The RED fouling monitor: a novel tool for fouling analysis, J. Membr. Sci. 570–571 (2019) 294–302.
[18] J. Moreno, V. Díez, M. Saakes, K. Nijmeijer, Mitigation of the effects of multivalent ion transport in reverse electrodialysis, J. Membr. Sci. 550 (2018) 155–162.
[19] J.W. Post, Blue Energy: Electricity Production From Salinity Gradients by Reverse Electrodialysis, Wageningen, Univ., 2009. Diss.
[20] M.A. de Lucas Pardo, D. Sarpe, J.C. Winterwerp, Effect of algae on flocculation of suspended bed sediments in a large shallow lake. consequences for ecology and sediment transport processes, Ocean Dyn. 65 (2015) 889–903.
[21] J. Bouchez, J. Gaillardet, C. France-Lanord, L. Maurice, P. Dutra-Maia, Grain size control of river suspended sediment geochemistry: clues from Amazon River depth profiles, Geochem. Geophys. Geosyst. 12 (2011) n/a-n/a.
[22] R.S. Wotton, EPS (Extracellular polymeric Substances), silk, and chitin: vitally important exudates in aquatic ecosystems, J. N. Am. Benthol. Soc. 30 (2011) 762–769.
[23] Environmental Protection Agency, EPA Water Treatment Manual - Filtration, 1995.
[24] A.H. Earn Tan, A.W. Ze Chew, A., Wing-keung law, deployment of recyclable polycarbonate as alternative coarse Media in Dual-media Rapid Filters, Energy Procedia 143 (2017) 475–480.
[25] APHA, Standard Methods for the Examination of Water and Waste Water: Method 2540 D, 21st ed., Water Environment Federation, Washington, 2005.
[26] G.A. O'Toole, L.A. Pratt, P.I. Watnick, D.K. Newman, V.B. Weaver, R. Kolter, Genetic approaches to study of biofilms, Methods Enzymol. 310 (1999) 91–109.
[27] S.J. Kassinger, M.L. van Hoek, Biofilm architecture: an emerging synthetic biology target, Synth. Syst. Biol. 5 (2020) 1–10.
[28] T. Suchecka, E. Biernacka, W. Piatkiewicz, Microorganism retention on microfiltration membranes, Filtr. Sep. 40 (2003) 50–55.
[29] N. Lebleu, C. Roques, P. Aimar, C. Causserand, Role of the cell-wall structure in the retention of bacteria by microfiltration membranes, J. Membr. Sci. 326 (2009) 178–185.
[30] Sara BinAhmed, Anissa Hasane, Zhaoxing Wang, Aslan Mansurov, Santiago Romero-Vargas Castrillón, Bacterial adhesion to ultrafiltration membranes: role of

hydrophilicity, natural organic matter, and cell-surface macromolecules, Environ. Sci. Technol. 52 (2018) 162–172.